arXiv:1610.04283v3 [cond-mat.mes-hall] 22 Oct 2016

Vortex-antivortex pairs induced by curvature

Smiljan Vojkovic,[1] Vagson L. Carvalho-Santos,[2] Jakson M. Fonseca,[3] and Alvaro S. Nunez[4]

[1]*Instituto de Física, Pontificia Universidad Católica de Chile, Campus San Joaquín Av. Vicuña Mackena 4860, Santiago, Chile.*

[2]*Instituto Federal de Educação, Ciência e Tecnologia Baiano - Campus Senhor do Bonfim, Km 04 Estrada da Igara, 48970-000 Senhor do Bonfim, Bahia, Brazil*

[3]*Universidade Federal de Viçosa, Departamento de Física, Avenida Peter Henry Rolfs s/n, 36570-000, Viçosa, MG, Brasil*

[4]*Departamento de Física, Facultad de Ciencias Físicas y Matemáticas, Universidad de Chile, Casilla 487-3, Santiago, Chile*

We show that the curvature of nanomagnets can be used to induce chiral textures in the magnetization field. Among the phenomena related to the interplay between geometry and magnetic behavior at nanomagnets, an effective curvature-induced Dzyaloshinskii-Moriya interaction has been recently predicted. In this work, it is shown that a magnetization configuration consisting of two structures with opposite winding numbers (vortex and antivortex) appear as remanent states. It is shown that these topological chiral configurations are a result of the Dzyaloshinkii-Moriya interaction induced by curvature. In this way, the obtained results present a new form to produce stable vortices and antivortices by using nanomagnets with variable curvature.

PACS numbers:

INTRODUCTION

Proper control over magnetization textures is at the heart of a large variety of technological applications. This makes of any new tool to control the fate of magnetization patterns a very interesting avenue for research. In this context, topological spin configurations such as chiral skyrmions, magnetic bubble domains, vortices and antivortices have been widely studied due to the possibility to produce devices based on magnonics and spintronics technology [1–12]. For example, skyrmion based "race-track" memory devices [4, 13] and vortex based transistor [14] have been recently proposed. Chiral skyrmions are two-dimensional topological solitons localized in nanoscale cylindrical regions [15–17]. The understanding of the physics of magnetic skyrmions and their applications in potential spintronic devices requires the knowledge of the properties of an isolated skyrmion. In this context, an analytical solution for isolated skyrmions has been recently obtained and compared with experimental results [18]. Despite vortices being also characterized by a winding number, in 3D systems they do not have topological stability and then, their stabilization in magnetic systems is ensured by subtle competition between the dipolar and exchange energies [19]. In this case, vortices can appear as the groundstate of submicron magnetic elements of different shapes [20–22]. In addition, vortex domain walls are stable configurations in cylindrical nanotubes and their dynamics is under intense investigation [24, 25]. Unlike skyrmions and vortices, the preparation of a nanostructure that contains a stable antivortex is a challenging task. Indeed, antivortices can appear as an unstable magnetization configuration during a vortex core reversal [26]. Nevertheless, experimental and theoretical works have reported that a stable single antivortex can appear in asterisk [9, 27] and cross-like [11] shaped permalloy particles. In this letter, we provide an additional mechanism for the nucleation, control and transport of chiral textures of the magnetization by appealing to the geometrical curvature of the system.

Curvature has become a cornerstone in the modern description of the behavior of magnetic systems. Indeed, a lot of effort has been dedicated to the understanding of the effects that the geometrical properties of a system have on the static and dynamic behavior of the magnetization [28]. For instance, Yershov *et al* have studied curved nanowires and they have shown that the presence of curvature and torsion [29–31] in such magnetic nanostructures yield the appearing of a domain wall pinning and a Walker limit [32] during the domain wall motion. The basics spin wave and domain wall motion physics behind the geometrical confinement of magnetic textures has been investigated in cylindrical nanomagnets [33–36] and a curvature-induced asymmetric spin wave has been predicted to appear in the spin wave dispersion along ferromagnetic nanotubes [37]. Finally, the coupling between an external magnetic field and the surface curvature can lead to the appeareance of a 2π-skyrmion excitation on magnetic surfaces described by the Heisenberg Hamiltonian [38, 39].

In a recent work, approximating the full extent of the dipolar interaction by a suitably chosen shape anisotropy, Gaididei *et al* [40] have obtained a functional to calculate the exchange energy for magnetic shells with an arbitrary geometry in function of its Gaussian and mean curvatures. They have shown that effective anisotropy and Dzyaloshinskii-Moriya interaction (DMI) [42, 43] are induced by curvature. Pylypovskyi *et al* showed that this curvature-induced DMI is responsible by a chiral symme-

try breaking of a domain wall motion in magnetic helices [44] and Möbius ring [45]. Based on the above and on the fact that the torus presents a curvature varying from negative (internal border) to positive (external border), with a relatively easy geometrical description, we propose that this shape is ideal to analyze the predicted chiral effects induced by the curvature. It is shown that the variable curvature of the torus yields chiral magnetization patterns with opposite winding numbers (vortex and antivortex) and so, a new way to stabilize vortices and antivortices in magnetic nanoparticles by using curvature effects is proposed. The magnetic properties of toroidal nanomagnets have been previously studied and it was shown that a torus can support a vortex as the groundstate for smaller sizes than cylindrical nanorings [46] and the hysteresis curves revealed two reversal modes for the magnetization [47]. Nevertheless, the geometrical parameters considered so far do not allow the appearance of more complex structures during reversal process that could evidence a curvature-induced DMI. Here, we study hollow toroidal nanoparticles that are expected to display the qualitative features rendered by the curvature-induced DMI [40].

THEORETICAL MODEL

In general, in a curved surface parametrized by the coordinates (q_1, q_2), we can write the magnetization an orthogonal curvilinear basis, $(\hat{q_1}, \hat{q_2}, \hat{n} = \hat{q_1} \times \hat{q_2})$, in the form $\vec{M} = M_S \mathbf{\Omega}$, with M_S being the saturation magnetization and

$$\mathbf{\Omega} = \hat{n} \cos\Theta + \hat{q_1} \sin\Theta \cos\Phi + \hat{q_2} \sin\Theta \sin\Phi \,, \qquad (1)$$

where, $\Theta \equiv \Theta(q_1, q_2)$ and $\Phi \equiv \Phi(q_1, q_1)$ describe the angles of the magnetization vector field in a curvilinear background. In this way, the exchange energy density for an arbitrary curved magnetic shell is explicitly written below [40, 41]

$$\mathcal{E}_{ex} = A \left[\sin\Theta(\nabla\Phi - \mathbf{\Xi}) - \cos\Theta \frac{\partial \mathbf{\Gamma}(\Phi)}{\partial \Phi} \right]^2 + \left[\nabla\Theta - \mathbf{\Gamma}(\Phi) \right]^2 \qquad (2)$$

where A is the stifness constant, $\mathbf{\Gamma}(\Phi)$ is a matrix depending on the Gauss and mean curvatures of the nanomagnet and $\mathbf{\Xi}$ is a modified spin connection.

A torus with genus 1 embedded in a 3D-space can be parametrized by

$$\vec{r} = (R + r\sin\theta)(\hat{x}\,\cos\varphi + \hat{y}\,\sin\varphi) + \hat{z}\, r\cos\theta \,, \qquad (3)$$

where R and r are respectively the toroidal and poloidal radii and θ plays the role of polar angle describing the torus surface (See Fig. 1). In this case, its Gaussian curvature is evaluated as $K = \sin\theta[r(R + r\sin\theta)]^{-1}$. The

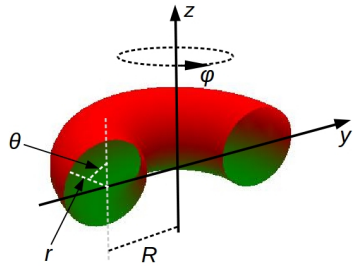

FIG. 1: Torus section showing the adopted coordinate system describing the torus external surface.

modified spin connection [40] can be calculated from the geometrical parameters defined in Eq. (3), leading to $\mathbf{\Xi} = -\hat{\varphi}\,\cos\theta(R + r\sin\theta)^{-1}$. It can be noted that the spin connection varies in function of θ in such way that $\mathbf{\Xi}(0) = -\hat{\varphi}/R$ and $\mathbf{\Xi}(\pi) = \hat{\varphi}/R$. In addition, by writing the gradient operator and the magnetization in a toroidal basis $(\hat{n} \equiv \hat{r}, \hat{q}_1 \equiv \hat{\theta}, \hat{q}_2 \equiv \hat{\varphi})$, the curvature-induced DMI energy density for an in-surface magnetization configuration [41] $(\Theta = \pi/2)$ is given by

$$\mathcal{E}_D = \frac{2\,A\,\cos\theta}{(R + r\sin\theta)^2} \partial_\varphi \Phi \,, \qquad (4)$$

From Eq. (4), one can estimate the effective DMI strenght induced by curvature. Indeed, we have that $\mathcal{D}/a^2 \sim A/R = J/Ra$ and thus, $\mathcal{D} \sim J(a/R)$, where a is the lattice constant and J is the exchange constant. From Eqs. (1) and (4), it can be noted that the effective DMI term to the energy of a in-surface vortex state, given by $\Theta = \pi/2$ and $\Phi = \pi/2$, and a single domain state, represented by $\Theta = \theta + \pi/2$ and $\Phi = \pi/2$ (pointing along x-axis direction), is 0 and then, no chiral effects are present for these magnetization fields. Nevertheless, due to its dependence on θ, effective DMI chiral effects coming from curvature must be evident when other magnetization configurations appearing in a toroidal nanomagnet are analyzed. Therefore, aiming to study metastable states in a toroidal nanomagnet and analyze the possibility of the appearance of chiral interactions induced by variable curvature, we have performed micromagnetic simulations for hollow Permalloy nanotori and solved the Landau-Lifshitz-Gilbert equation [48, 49].

RESULTS

The LLG equation was solved by using the 3D Object Oriented MicroMagnetic Framework (OOMMF) [50] package using the computational facilities available in nanohub [51]. The simulations were run using an exchange constant $A = 1.3 \times 10^{-11}$ J/m, a saturation magnetization $M_S = 860$ A/m, a cubic mesh with size 1 nm and a damping $\alpha = 0.5$. The considered geometric parameters are: toroidal radius $R = 52$ nm; internal

poloidal radius $r_i = 20$ nm; and external poloidal radius $r_e = 26$ nm, resulting in a 6 nm thickness torus. In the simulations, we have saturated the magnetizatin with an external magnetic field in such way that the initial state consists in a single domain along x-axis direction. Then, we have diminished the magnetic field until 0 and analyzed the remanent state of the magnetization.

Fig. 2a presents the obtained configuration and the appearance of a vortex at the external torus border is evident. Aiming to analyze the magnetization at the internal borders we have done four cutoffs highlighted in the planes showed in Fig. 2a. Fig. 2b shows a representation of the obtained magnetization configuration, given by the in-plane VA ansatz, $\Phi = \arg[r\cos\theta + i(R + r\sin\theta)\cos(\varphi \mp \pi/2)]$. The signals $-(+)$ are related to the interval of the azimuthal angle, that is, $-$ for $\varphi \in [-\pi/4, \pi/4]$ and $+$ for $\varphi \in [3\pi/4, 5\pi/4]$. From Figs. 2c-f, it can be observed the formation of two vortices state with opposite chiralities at the external borders (positive curvature) of the torus and antivortices, also with opposite chiralities, at the internal borders (negative curvature) of the torus. The antivortex is the topological counterpart of a vortex, having opposite winding number and so, the appearing of two pairs vortex-antivortex (VA) preserves the topological winding number of the initial state ($Q = 0$ for a single domain). In fact, while a vortex has winding number $Q_v = +1$, an antivortex presents $Q_a = -1$. The conservation of the winding number occurs because two configurations belonging to different homotopy classes cannot be continuously deformed one to another [52] and thus, isolated vortices (antivortices) or two pairs of vortices (antivortices) are not possible in this case. In addition, the two VA pair state demands lower energy than a two vortices pairs state since if a two pair of vortices would be the remanent state, four antivortices must appear at $\theta = 0(\pi)$ $\phi = 0(\pi)$ in order to smoothly connect such vortices pairs, increasing the dipolar and exchange energy of the system. Between each VA pair, it can be noted an onion state along the torus that is, the remanent state consists in an onion state connecting two VA pairs. In addition, it can be noted that each VA has opposite chirality, that is, if the vortex at the external surface has positive chirality, its antivortex counterpart presents a negative chirality, evidencing the dependence of the signal of the effective curvature-induced DMI on the curvature of the magnetic particle. From the used geometrical parameters, one can estimate the curvature-induced DMI effective strengh in $\mathcal{D} \sim 0.005 - 0.012$ meV. Due to the fact an antivortex is found at the internal border of the torus, one can conjecture that the antivortex is for a negative curvature as the vortex is for a positive curvature [53]. The study on the magnetic groundstate of particles with negative curvature is still lacking.

In order to show that the metastable state appearing during the reversal process of the magnetization on a hollow torus is a result of a curvature-induced DMI, we have performed micromagnetic simulations for a hollow cylinder with same geometrical dimensions of the torus. By observing the remanent state given in Fig 3a, it can be noted that a single vortex turning around the ring hole is the remanent state and chiral metastable states do not appear in this case. Indeed, from parametrizing a ring in a polar coordinate system, the modified spin connection for the cylindrical geometry is evaluated as $\boldsymbol{\Xi} = 0$ and thus, there is not a curvature-induced DMI term to the magnetic energy in this case (consequently no chiral configuration is noted). Thus, we can state that the metastable states appearing during the reversal process of the magnetization in a hollow torus, evidenced in Fig.2, are a result of an effective DMI induce by curvature, as predicted by Gaididei *et al* [40].

The formation of VA on a toroidal shell is a very interesting result, as from the fundamental as from the applied point of view. From the fundamental Physics point of view, the appearing of a configuration with positive winding number at the external border and a configuration with negative winding number at the internal border of the torus evidence the intrinsic relationship between curvature and magnetization properties of ferromagnetic nanoparticles. Then, one can conclude that besides of a curvature-induced DMI, there is the possibility of the appearing of a curvature-induced topological metastable state in curved nanomagnets. From the applied point of view, if it is possible to generate and guide the VA state from a curved section of a nanowire to a straight section without annihilate them, this pair could be thought as a candidate to compose devices based on the concept of spin logic operations [6] or "race-track" memory [54]. Another interesting possibility is to study the interaction of this pair vortex-antivortex with oscillating magnetic fields aiming to use these chiral states as nano-emiter/nano-collector (nanoantena) devices [55, 56].

We have also studied the behavior of the magnetization in a hollow toroidal and cylindrical nanomagnets by analyzing the remanent state when an external magnetic field is applied along z-axis direction. In remanence, it can be noted the formation of a double vortex with opposite chirality (See Fig. 4). It can be noted that due to the smooth curvature of the torus, the vortex state is still present at its internal neck while in the cylindrical case. On the other hand, due to the high exchange energy cost to support a vortex, the internal neck of the hollow cylindrical ring presents a single domain state pointing along z-axis direction (See Fig. 3b). For both cases, the formation of a two opposite vortex state can be explained by the need to reduce the dipolar energy (vortices with same chirality would lead to larger dipolar energy) and the nanomagnets behave as an array of nanorings separated by a vertical distance d [57]. The two vortices remanent state is also very interesting for applications in spintronic and magnonic devices, due to the possibility to control the chirality of the vortex on one side of the

nanomagnet by controlling the other one.

The reversal process of the magnetization has been analyzed aiming to understand the mechanism behind the nucleation and annihilation of the observed VA pair (H_x) and two opposite vortices (H_z). The hysteresis curves describing such reversal processes is shown in Fig. 5. It is observed that when the magnetic field is applied along x-axis direction, the hysteresis curve presents a reduction in the magnetization at remanence. This reduction evidences the formation of the two VA pairs. Fom the analysis of a video available in Supplemental Materials [58], it is observed that as the magnetic field increases in the opposite direction, each VA pair annihilate giving place to a transient state formed by two in-surface domain walls at the opposite sides of the torus. These domain walls joint thamselves and the hysteresis curve present a typical neck associated to the nucleation of a vortex state. For $|H_x| \geq 100$ mT, the vortex configuration gives place again to a double domain wall, which diminish their lenghts when the magnetic field continues to increase, disappearing for $H_x \approx 250$ mT. On the other hand, Fig 5b describes the hysteresis curve when the magnetic field is applied along z-axis direction. It can be noted a fast decreasing in the magnetization for $H \leq 500$ mT, evidencing the formation of the opposite vortices with a small region in which magnetization points along z-axis. These vortices remain at remanence and are annihilated at $|H_z| \approx 100$ mT.

It is important to note that in both cases (in-plane and out-of-plane magnetic fields), the magnetic field strenght that annihilates the remanent state is small (in the order of 200 mT) and thus, the obtained metastable states are easily nucleated and annihilated. Thus, the creation and annihilation of a VA state in toroidal nanotubes could be used in data storage devices.

CONCLUSIONS

In conclusion, chiral topological interactions induced by curvature can take place in a hollow nanomagnet with variable curvature. Due to its variable curvature, the remanent state of the magnetization in a hollow torus consists in a configuration in which a vortices appear at the external borders and antivortices are present at the internal border of the torus. Qualitative analysis supports the fact that a VA state has lower energy than a state in which the torus presents two pairs of vortices. From a direct comparison of the results obtained for a geometry with variable curvature with the remanent state of a hollow cylindrical nanomagnet (Gaussian curvature is 0), we showed that the VA state is a result of an effective DMI induced by curvature. In this case, we have shown the new possibility to stabilize vortices and antivortices in magnetic nanoparticle by using curvature. This chiral state could be used in devices working under the concept of spintronic, race-track memory and nanoantenas. Finally, the remanent state when the external magnetic field is pointing along z-axis direction consists in a two vortice state with opposite chirality. In this case, main differences between toroidal and cylindrical cases live in the vortex structure in the internal border of both geometries. The reversal processes for both cases (**H** pointing along x and z direction) were analyzed. The machanism behind the appearance and annihilation of the VA pairs have been described by analyzing the hysteresis curves and it was shown that the VA pairs annihilate themselves and the reversal process is followed by the nucleation of a single vortex state.

Acnowledgements: The authors would like to thank the Brazilian agencies CNPq and Fapemig, for financial support. ASN would like to thank funding from grant Fondecyt 1150072. ASN also acknowledges support from Financiamiento Basal para Centros Científicos y Tecnológicos de Excelencia, under Project No. FB 0807 (Chile). We are gratefull to J. Otálora and A. Bogdanov for their valuable comments on our work.

[1] S. Woo, K. Litzius, B. Krüger, M.-Y. Im, L. Caretta, K. Richter, M. Mann, A. Krone, R.M. Reeve, M. Weigand, P. Agrawal, I. Lemesh, M.-A. Mawass, P. Fischer, M. Kläui, and G.S.D. Beach, Nat. Mater. **15**, 501 (2016).

[2] C. Moreau-Luchaire, C. Moutafis, N. Reyren, J. Sampaio, C.A.F. Vaz, N. VanHorne, K. Bouzehouane, K. Garcia, C. Deranlot, P. Warnicke, P. Wohlhüter, J.-M. George, M. Weigand, J. Raabe, V. Cros, and A. Fert, Nat. Nanotech. **11** 444.

[3] N.S. Kiselev, A.N. Bogdanov, R. Schäfer, and U.K. Röβler, J. Phys. D: Appl. Phys. **44**, 392001 (2011).

[4] A. Fert, V. Cros, and J. Sampaio, Nature Nanotech **8**, 152 (2013).

[5] J. Sampaio, V. Cros, S. Rohart, A. Thiaville, and A. Fert, Nat. Nanotech. **8**, 839 (2013).

[6] S.B. Choe, Y. Acremann, A. Scholl, A. Bauer, A. Doran, J. Stohr, and H.A. Padmore, Science **304**, 420 (2004).

[7] R. Hertel, S. Gliga, M. Fähnle, and C.M. Schneider, Phys. Rev. Lett. **98**, 117201 (2007).

[8] Q.F. Xiao, J. Rudge, B.C. Choi, Y.K. Hong, and G. Donohoe, Appl. Phys. Lett. **89**, 262507 (2006).

[9] S. Gliga, M. Yan, R. Hertel, and C.M. Schneider, Phys. Rev. **B 77**, 060404(R) (2008).

[10] H. Wang, and C.E. Campbell, Phys. Rev. **B 76**, 220407(R) (2007).

[11] V.L. Mironov, O.L. Ermolaeva, S.A. Gusev, A.Y. Klimov, V.V. Rogov, B.A. Gribkov, O. G. Udalov, A.A. Fraerman, R. Marsh, C. Checkley, R. Shaikhaidarov, and V.T. Petrashov, Phys. Rev. **81**, 094436 (2010).

[12] A Roldán-Molina, A S Nunez and J Fernández-Rossier, New J. Phys. **18**, 045015 (2016)

[13] R. Tomasello, E. Martinez, R. Zivieri, L. Torres, M. Carpentieri, and G. Finocchio, Sci. Rep. **4**, 6784 (2014).

[14] D. Kumar, S. Barman, and A. Barman, Sci. Rep. **4**, 04108 (2014).

[15] A.N. Bogdanov, and D.A. Yablonskii, Sov. Phys. JETP **68**, 101 (1989).

[16] A. Bogdanov, and A. Hubert, J. Magn. Mag. Mat. **195**, 182 (1999).

[17] U.K. Roβler, A.N. Bogdanov, and C. Pfleiderer, Nature **442**, 797 (2006)

[18] A.O. Leonov, T.L Monchesky, N. Romming, A. Kubetzka, A.N. Bogdanov, and R. Wiesendanger, New J. Phys. **18**, 065003 (2016).

[19] K.L. Metlov, K.Y. Guslienko, J. Magn. Mag. Mat. **242**, 1015 (2002).

[20] T. Shinjo, T. Okuno, R. Hassdorf, K. Shigeto, and T. Ono, Science **289**, 930 (2000).

[21] N.A. Usov, and S.E. Peschany, J. Magn. Magn. Mater. **118**, L290 (1993).

[22] C. Rawlings, S. Weigelt, B. Hong, C.H. Barnes, M.E. Welland, and C. Durkan, Phys. Rev. **B 82**, 085404 (2010).

[23] V.L. Carvalho-Santos, R.G. Elias, J.M. fonseca, and D. Altbir, J. Appl. Phys. **117**, 17E518 (2015).

[24] J.A. Otálora, J.A. López-López, P. Vargas, and P. Landeros, Appl. Phys. Let. **100**, 072407 (2012).

[25] J.A. Otálora, J.A. López-López, P. Vargas, A. S. Núñez, and P. Landeros, J. Magn. Mag. Mat., 341, 86-92 (2013).

[26] B.V. Waeyenberge, A. Puzic, H. Stoll, K. W. Chou, T. Tyliszczak, R. Hertel, M.Fähnle, H. Brückl, K. Rott, G. Reiss, I. Neudecker, D. Weiss, C. H. Back, and G. Schütz, Nature **444**, 461 (2006).

[27] K. Shigeto, T. Okuno, K. Mibu, T. Shinjo, and T. Ono, Appl. Phys. Lett. **80**, 4190 (2002).

[28] R. Streubel, P. Fischer, F. Kronast, V.P. Kravchuk, D.D. Sheka, Y. Gaididei, O.G. Schmidt, and D. Makarov, J. Phys. **D 49**, 363001 (2016).

[29] K.V. Yershov, V.P. Kravchuk, D.D. Sheka, and Y. Gaididei, Phys. Rev. **B 92**, 104412 (2015).

[30] D.D. Sheka, V.P. Kravchuk, K.V. Yershov, and Y. Gaididei, Phys. Rev. **B 92**, 054417 (2015).

[31] K.V. Yershov, V.P. Kravchuk, D.D. Sheka, and Y. Gaididei, Phys. Rev. **B 93**, 094418 (2016).

[32] N.L. Schryer, and L.R. Walker, J. Appl. Phys. **45**, 5406 (1974).

[33] C.A. Ferguson, D.A. MacLaren, and S. McVitie, J. Magn. Mag. Mat. **381**, 457 (2015).

[34] A.L. González, P. Landeros, Á.S. Núñez, J. Magn. Mag. Mat. **322**, 530 (2010).

[35] P. Landeros, and Á.S. Núñez, J. Appl. Phys. **108**, 033917 (2010).

[36] J.A. Otálora, J.A. López-López, A.S. Núñez, and P. Landeros, J. Phys.: Cond. Mat. **24**, 436007 (2012).

[37] J.A. Otálora, M. Yang, H. Schultheiss, R. Hertel, and A. Kákay, Phys. Rev. Lett., Accepted (2016).

[38] V.L. Carvalho-Santos, R.G. Elias, D. Altbir, and J.M. Fonseca, J. Magn. Mag. Mat. **391**, 179 (2015).

[39] V.L. Carvalho-Santos, and Rossen Dandoloff, Phys. Lett. **A 376**, 3551 (2012).

[40] Y. Gaididei, V.P. Kravchuk, and D.D. Sheka, Phys. Rev. Lett. **112**, 257203 (2014).

[41] D.D. Sheka, V.P. Kravchuk, and Y. Gaididei, J. Phys. A: Math. Theor. **48**, 125202 (2015).

[42] I.E. Dzyaloshinskii, JETP **10**, 628 (1960).

[43] T. Moriya. Phys. Rev. **120**, 91 (1960).

[44] O.V. Pylypovskyi, D.D. Sheka, V.P. Kravchuk, K.V. Yershov, D. Makarov, and Y. Gaididei, Sci. Rep. **6**, 23316 (2016).

[45] O.V. Pylypovskyi, V.P. Kravchuk, D.D. Sheka, D. Makarov, O.G. Schmidt, and Y. Gaididei, Phys. Rev. Lett. **114**, 197204 (2015).

[46] V.L. Carvalho-Santos, W.A. Moura-Melo, and A.R. Pereira, J. Appl. Phys. **108**, 094310 (2010).

[47] S. Vojkovic, A.S. Nunez, D. Altbir, and V.L. Carvalho-Santos, J. Appl. Phys. **120**, 033901 (2016).

[48] L. Landau and E. Lifshitz, Ukr. J. Phys. **53**, 14 (2008); Reprinted from Phys. Zeitsch. der Sow. **8**, 153 (1935).

[49] T. L. Gilbert, IEEE Trans. Magn. **40**, 3443 (2004).

[50] M. J. Donahue and D. G. Porter, National Institute of Standards and Technology Interagency Reports NISTIR No. 6376, 1999.

[51] Michael Joseph Donahue; Donald Gene Porter; Zachary Yu (2016), "OOMMF: Object Oriented MicroMagnetic Framework," https://nanohub.org/resources/oommf. (DOI: 10.4231/D34X54H8T).

[52] R. Rajaraman, Solitons and Instantons: An Introduction to Quantum Field Theory (North-Holland, Amsterdam, 1984).

[53] D.D. Sheka, V.P. Kravchuk, M.I. Sloika, and Y. Gaididei, SPIN **3**, 1340003 (2013).

[54] S.S.P. Parkin, M. Hayashi, and L. Thomas, Science 320, 190 (2008).

[55] M.A. Suarez, T. Grosjean, D. Charraut, and D. Courjon, Opt. Comm. **270**, 447 (2007).

[56] N. Caselli, F.L. China, W. Bao, F. Riboli, A. Gerardino, L. Li, E.H. Linfield, F. Pagliano, A Fiore, P.J. Schuck, S. Cabrini, A. Weber-Bargioni, M. Gurioli, and F. Intonti, Sci. Rep. **5**, 9606 (2015).

[57] J. Escrig, P. Landeros, D. Altbir, M. Bahiana, J. D'Albuquerque e Castro, Appl. Phys. Lett. **89**, 132501 (2006).

[58] See supplemental materials for a video showing the reversal process of the VA pair.

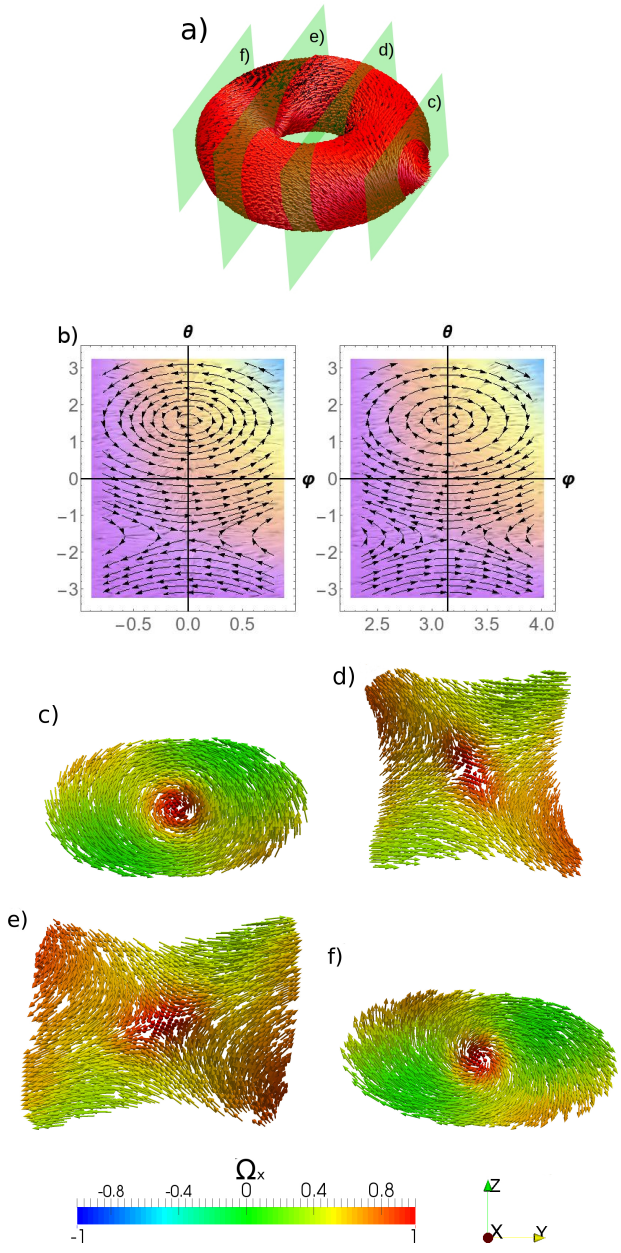

FIG. 2: Snapsot of the remanent state of the magnetization when an external magnetic field is applied along x-axis direction. Fig. a shows the remanent state evidencing the presence of a vortex at the external border of the torus. Fig. b consists in a representation of the magnetization in function of θ and φ aiming to show the in-surface component of VA pair. Figs. c, d, e and f show a front view of the planes represented in the Fig.a. These highlighted planes evidence the appearing of a vortex at the external border of the torus (c and f) and the anti-vortex at the internal border (d and e).

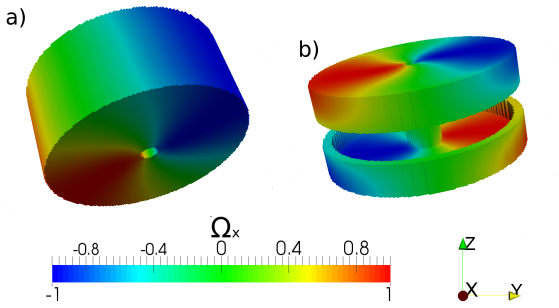

FIG. 3: Remanent state for a holow cylindrical nanoparticle when the magnetic field is pointing along x-axis direction (a) and z-axis direction (b).

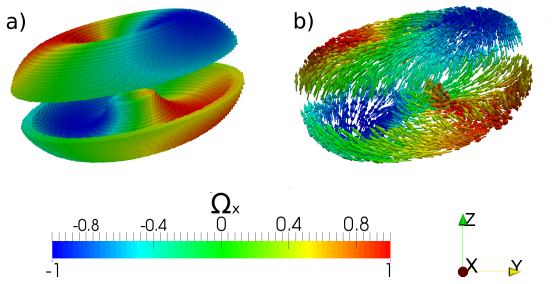

FIG. 4: Remanent states of toroidal nanoparticle when an out-of-plane magnetic field is applied.

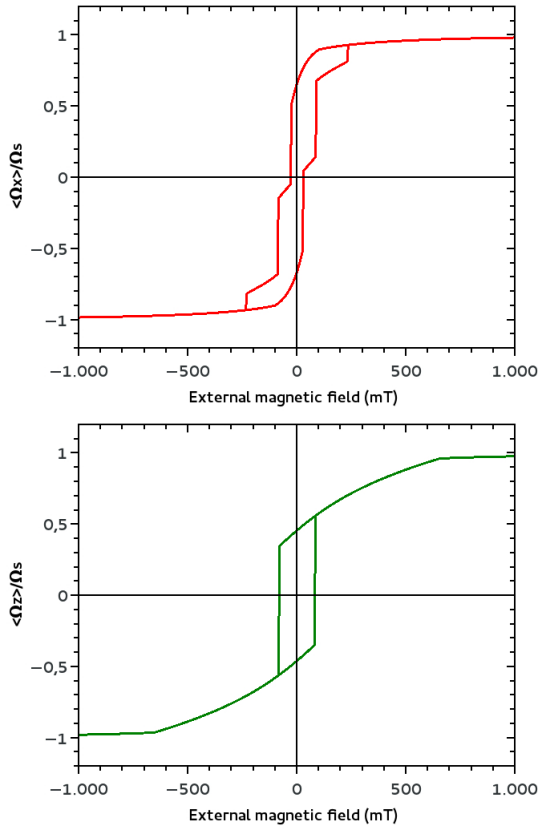

FIG. 5: Hysteresis curves of reversal processes when an in-plane (a) and an out-of-plane (b) magnetic fields are applied into the system.